Dispersion Coefficient for Laminar Flow in Curved Tubes

The axial dispersion coefficient in a fluid in laminar flow in a tube is generally smaller in a curved tube than in a straight tube, because of the enhancement of lateral transport by secondary flows. In this paper the extent of this reduction is computed using Horn's modification of Aris's method of moments. Dimensional analysis suggests that the most convenient form in which to represent the results is that obtained empirically by Trivedi and Vasudeva. The results presented here cover the whole laminar flow regime, and show the region of applicability of previously computed dispersion coefficients to be limited. The computed dispersion coefficients agree well with previously reported experimental results for small Schmidt numbers; however, discrepancies are present at large Schmidt numbers. Possible causes are discussed.

Ph. Daskopoulos, A. M. Lenhoff
Department of Chemical Engineering
University of Delaware
Newark, DE 19716

Introduction

The axial dispersion of a solute in a fluid in laminar flow in a tube is caused by the nonuniform velocity profile across the cross section; the evolution of the axial area-average concentration profile is, however, also affected by the action of lateral diffusion. Taylor (1953, 1954) and Aris (1956) showed that for dispersion in a straight tube of circular cross section the balance between the two effects causes the area-average concentration profile to become Gaussian in shape sufficiently far downstream. The process can thus be described using a Fickian mechanism, with the Taylor-Aris dispersion coefficient ϵ related to the molecular diffusivity $\mathcal{D}$ by

$$\frac{\epsilon}{\mathcal{D}} = 1 + \frac{Pe^2}{192} \tag{1}$$

where $Pe = 2W_m a/\mathcal{D}$ is a Peclet number. The condition for applicability of Eq. 1 follows from the requirement for sufficient time for molecular diffusion across the cross section; this requires the tube length to be $L \gg W_m a^2/\mathcal{D}$.

In the case of a curved tube, the curvature induces secondary flows that enhance lateral mixing and hence tend to reduce the extent of dispersion from that described by Eq. 1. This is relevant to dispersion in, for instance, heating or cooling coils. Of perhaps greater quantitative importance, however, is that Eq. 1 is the basis for a technique for measuring diffusivities in fluids. In practice, particularly in liquid systems, the tube lengths required for Eq. 1 to hold are so great that coiled tubes are usually needed (Pratt and Wakeham, 1974, 1975), making the use of this equation suspect.

That the secondary flows may reduce dispersion was apparently first recognized at about the same time by van Andel et al. (1964) and Koutsky and Adler (1964), who demonstrated the effect experimentally. Only the gas-phase experiments reported by the first group yielded Gaussian concentration profiles for laminar flow systems, however, so that the corresponding dispersion coefficients were the first reported for curved tubes. More recent experimental results include those of Trivedi and Vasudeva (1975), Nigam and Vasudeva (1976), Shetty and Vasudeva (1977), and van den Berg and Deelder (1979).

Several theoretical studies have sought to predict dispersion coefficients in curved tubes; these have been limited by the descriptions of both the hydrodynamics and the mass transfer in the problem. The hydrodynamic characteristics were first considered by Dean (1927, 1928), and most subsequent work has followed his example of considering only tubes of negligible curvature, $\delta = a/R$. This assumption leaves the so-called Dean number $\kappa = \sqrt{\delta Re}$ as the single parameter characterizing the flow. Dean used a perturbation method to examine low Dean number flows, but more recent work has been predominantly numerical. Berger et al. (1983) provide an extensive review of the effect of κ on the flow behavior, with more recent results summarized by Daskopoulos and Lenhoff (1988). The essential features of the flow comprise a distorted Poiseuille-like axial flow together with a pair of counterrotating secondary flow vortices, increasing in intensity with κ. A four-vortex flow is also

possible at higher κ, but it is not relevant to the present discussion.

Erdogan and Chatwin (1967), using intuitive arguments based on those of Taylor (1953) for straight tubes, used Dean's (1927) velocity distribution to obtain an asymptotic expression for the dispersion coefficient valid at low Dean numbers. As expected, the predicted effect was that the secondary flows generally reduce the dispersion coefficient. However, for sufficiently small Schmidt numbers increased dispersion coefficients can result from the higher maximum axial velocity in the curved tube relative to that in the straight tube. Nunge et al. (1972) extended these results using the analytical dispersion model of Gill (1967); since their results were based on the velocity distribution of Topakoglu (1967), which extended Dean's expansion to include the effects of curvature, the effect of curvature was also incorporated in the asymptotic result. The Erdogan and Chatwin result represents the small curvature limit of the Nunge et al. result; for larger curvatures a significant difference is seen mainly for small Schmidt numbers. However, since the Topakoglu hydrodynamic description is only to second order in curvature, some of the results shown by Nunge et al. for tightly coiled tubes may be in a part of the parameter space for which their results are not reliable.

The Erdogan and Chatwin and the Nunge et al. results predict a relatively sharp transition from straight-tube to negative dispersion coefficients at finite values of Dean and Schmidt numbers; no indication is given as to the upper limit of applicability of the results. Janssen (1976) also began with Dean's hydrodynamic results, but showed that appropriate scaling in this regime leaves $\kappa^2 Sc$ as the only dimensionless parameter in the problem. Janssen then used a numerical implementation of Taylor's method in showing that, while the dispersion coefficient indeed falls rapidly at first, it appears to level off at a finite value at high $\kappa^2 Sc$ when plotted as a fraction of its straight-tube value. Johnson and Kamm (1986) used a similar approach but a more accurate computational procedure. Their results are qualitatively similar to Janssen's, and separate high Sc calculations confirmed that the high $\kappa^2 Sc$ asymptote is at 0.2 of the straight-tube dispersion coefficient.

Other related work is that of McConalogue (1970), who used the velocity distribution of McConalogue and Srivastava (1968) to examine the purely convective contribution to the distribution of residence times. Ruthven (1971) reported corresponding results for Dean's velocity distribution.

The work of Nunge et al. (1972) discussed above probably represents an upper limit on the feasibility and utility of analytical approximations for dispersion coefficients. In the present work dispersion coefficients are determined numerically over a much wider range of Dean numbers than has previously been examined theoretically, although the restriction to loosely coiled tubes is retained. The method used is that of Horn (1971), which is a modification of the method of moments of Aris (1956).

Problem Statement

Horn's (1971) method applies to long systems of which the cross-sectional geometry and hydrodynamic characteristics are unchanged along the principal axis. It extends Aris's (1956) method of moments to show that the dispersion coefficient can be found by solving, in the cross-sectional plane, a steady-state convective diffusion problem which for present purposes can be written as

$$v_s \cdot \nabla_s \psi = \mathcal{D} \nabla_s^2 \psi + W - W_m \tag{2}$$

where the subscript s denotes a quantity in the cross-sectional plane. Equation 2 describes the distribution in the plane of a solute produced by a source distributed as the local axial velocity, W, relative to its area average. There is thus no net source, as reflected also in the use of no-flux conditions at the lateral boundaries. The solution ψ of Eq. 2, which has units of length, allows the dispersion coefficient to be found by quadrature in the plane,

$$\frac{\epsilon}{\mathcal{D}} = 1 + \frac{1}{A} \int_A \nabla_s \psi^T \cdot \nabla_s \psi \, dA \tag{3}$$

with the first term on the righthand side representing the molecular diffusion contribution. Brenner (1980) has extended Horn's development to permit the determination of dispersion coefficients in three-dimensional spatially periodic systems.

Horn's analysis can be applied to dispersion in fully developed pressure-driven flow in curved ducts, using an orthogonal toroidal system of coordinates, Figure 1. The center of the coordinate system is fixed at the center of the curved tube and the coordinates of any point P are denoted by (r', α, θ), with the gradient operator

$$\nabla \equiv \left(\frac{\partial}{\partial r'}, \frac{1}{r'} \frac{\partial}{\partial \alpha}, \frac{1}{1 + \frac{r'}{R} \cos \alpha} \frac{\partial}{\partial (R\theta)} \right) \tag{4}$$

The flow, with velocity components (U, V, W), is caused by a constant axial pressure gradient $G = R^{-1}(\partial p / \partial \theta)$. For steady, fully developed flow the velocity components are independent of axial position as expressed by θ, so that the primary (axial) flow is locally rectilinear, and the secondary flow provides the planar velocity v_s, with components U and V, in Eq. 2. Further details

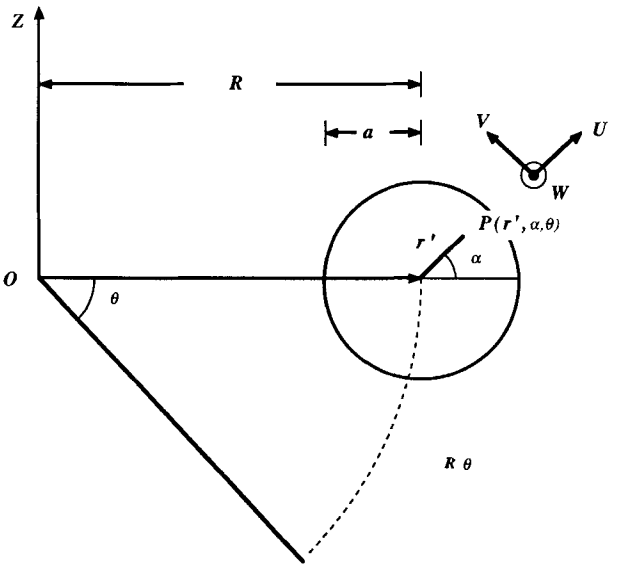

Figure 1. Toroidal coordinate system.

regarding the hydrodynamic problem may be found elsewhere (Berger et al., 1983; Daskopoulos and Lenhoff, 1988).

The convective diffusion problem, Eq. 2, specialized to the physical situation at hand for tubes of negligible curvature, becomes

$$U\frac{\partial\psi}{\partial r'}+\frac{V}{r'}\frac{\partial\psi}{\partial\alpha}=\mathcal{D}\left(\frac{\partial^2\psi}{\partial r'^2}+\frac{1}{r'}\frac{\partial\psi}{\partial r'}+\frac{1}{r'^2}\frac{\partial^2\psi}{\partial\alpha^2}\right)+W-W_m \quad (5)$$

where W_m is the area-average axial velocity. Equation 5 is to be solved subject to no-flux boundary conditions at the walls,

$$\frac{\partial\psi}{\partial r'}=0 \quad \text{at} \quad r'=a \quad (6)$$

and symmetry about the central plane of the pipe (OC in Figure 1),

$$\frac{\partial\psi}{\partial\alpha}=0 \quad \text{at} \quad \alpha=0,\pi \quad (7)$$

$$\frac{\partial\psi}{\partial r'}=0 \quad \text{at} \quad r'=0, \quad \text{for} \quad \alpha=\frac{\pi}{2} \quad (8)$$

Equations 5 to 8 can be rewritten in dimensionless form by introducing the scaled variables and parameters

$$r=\frac{r'}{a};\quad u=\frac{aU}{\nu};\quad v=\frac{aV}{\nu};\quad w=\frac{aW}{\nu}\sqrt{\delta};$$

$$\kappa=\sqrt{\delta}\frac{2aW_m}{\nu}=\sqrt{\delta}Re;\quad \beta=\frac{\psi}{aReSc} \quad (9)$$

The velocities are scaled so as to render centrifugal effects similar in magnitude to inertial and viscous effects in the secondary flow; the dimensionless velocity components are dependent on a single parameter, the Dean number, κ. The scaled convective diffusion equation and boundary conditions are

$$\kappa Sc\left(u\frac{\partial\beta}{\partial r}+\frac{v}{r}\frac{\partial\beta}{\partial\alpha}\right)=\kappa\left(\frac{\partial^2\beta}{\partial r^2}+\frac{1}{r}\frac{\partial\beta}{\partial r}+\frac{1}{r^2}\frac{\partial^2\beta}{\partial\alpha^2}\right)+w-\frac{\kappa}{2} \quad (10)$$

$$\frac{\partial\beta}{\partial r}=0 \quad \text{at} \quad r=1 \quad (11)$$

$$\frac{\partial\beta}{\partial\alpha}=0 \quad \text{at} \quad \alpha=0,\pi \quad (12)$$

$$\frac{\partial\beta}{\partial r}=0 \quad \text{at} \quad r=0, \quad \text{for} \quad \alpha=\frac{\pi}{2} \quad (13)$$

from which it is apparent that the only parameters on which the dimensionless concentration, β, is dependent are κ and Sc. This dependence would result even without the Schmidt number present in the definition of β in Eq. 9, but the form chosen results in a more convenient expression for the dispersion coefficient, as explained below.

The solution $\beta(r,\alpha)$ of Eqs. 10 to 13 may be used in the dimensionless form of Eq. 3 to evaluate the dispersion coefficient:

$$\frac{\epsilon}{\mathcal{D}}=1+\frac{Pe^2}{\pi}\int_0^1\int_0^{2\pi}\left\{\left(\frac{\partial\beta}{\partial r}\right)^2+\left(\frac{1}{r}\frac{\partial\beta}{\partial\alpha}\right)^2\right\}r\,dr\,d\alpha \quad (14)$$

This result, and hence the choice of scaling in Eq. 9, is useful for two reasons. First, β is a function of κ and Sc only, and is not dependent on the curvature, δ, explicitly. Since $Pe = ReSc$, the factor Pe^2 can be written as $(\kappa Sc)^2/\delta$, so the effect of curvature on the scaled dispersion coefficient $\epsilon/\mathcal{D}$ is given directly by the factor $1/\delta$ premultiplying the integral in Eq. 14. The second reason Eq. 14 is convenient is that for straight tubes the integral is independent of all dimensionless parameters, and Eq. 14 explicitly shows the familiar Pe^2 dependence as in Eq. 1. These observations will be useful in presenting results later.

Solution Procedure

The velocity profiles for use in Eq. 10 were obtained by an orthogonal collocation procedure, as described in detail elsewhere (Daskopoulos and Lenhoff, 1988). For the diffusion equation 10, too, orthogonal collocation (or another global weighted residual method) is suitable because the system has boundaries described explicitly in terms of coordinate surfaces. This method also has the advantage that it provides a continuous function as a solution over the entire computational domain, making the differentiation and quadrature required by Eq. 14 straightforward. The basis functions used for the diffusion problem were Fourier series in the azimuthal direction, due to the periodicity of the problem, and Chebyshev polynomials in the radial direction, in order to minimize the maximum error of the interpolation (Lanczos, 1956).

Because of the symmetry along the central plane the computational domain can be reduced to the upper semicircular region of the tube cross section, $0 \le r \le 1$, $0 \le \alpha \le \pi$. Within this domain, Eq. 10 was solved by substituting for β an expansion satisfying the constraints imposed by the boundary conditions and system geometry:

$$\begin{aligned}\beta=(1-r^2)^2\sum_{i=0}^{N}\beta_{2i,0}&\left\{P_{2i}(r)-\frac{P'_{2i}(1)}{P'_{2(N+1)}(1)}P_{2(N+1)}(r)\right\}\\&+(r^4-2r^2)\sum_{i=1}^{N}\sum_{j=0}^{M}\beta_{2i,2j}\\&\cdot\left\{P_{2i}(r)-\frac{P'_{2i}(1)}{P'_{2(N+1)}(1)}P_{2(N+1)}(r)\right\}\cos(2j\alpha)\\&+\sum_{i=0}^{N}\sum_{j=0}^{M}\beta_{2i+1,2j+1}\\&\cdot\left\{P_{2i+1}(r)-\frac{P'_{2i+1}(1)}{P'_{2(N+1)+1}(1)}P_{2(N+1)+1}(r)\right\}\\&\cdot\cos((2j+1)\alpha). \quad (15)\end{aligned}$$

Here $P_k(r)$ are Chebyshev polynomials of order k and a prime denotes differentiation with respect to r. For a given expansion order (N, M), the residuals are set to zero at a set of collocation points to obtain a linear algebraic system of $2(N+1)(M+1)$ equations, from which the coefficients in the expansion, Eq. 15, can be found by standard methods. The collocation points used

were the roots of the orthogonal function sets in the trial solution. The criterion used to characterize a solution as converged was based on the relative improvement in the value of the quadrature in Eq. 14 resulting from an increase in the order of the expansion in Eq. 15. A typical requirement for indicating that the expansion was of sufficiently high order was that the quadrature of Eq. 14 not change by more than 0.5% between two successive approximations. Another check came from monitoring the smoothness of the distribution of the concentration β in the computational domain.

The numerical technique was used over a wide range of Peclet numbers. For small Pe (of the order of 100) an expansion with $N = 5$, $M = 4$ is adequate and requires much less than 1 s CPU time on a DEC VAX 11/785 computer. This increases for $Pe = O(10{,}000)$ to typical values of $N = 16$, $M = 11$(~2–3 s CPU time), and to even larger expansions as Pe increases, because of steep concentration gradients in regions where convective transport is weak. Convergence problems were most apparent near the center of the secondary flow vortex, as indicated by wiggles in the contours of β. After unsuccessful attempts to accelerate convergence by a transformation stretching the radial coordinate, the convection-dominated cases ($Pe \geq 150{,}000$) were solved on a Cray X-MP/48 computer, where a typical run required 20–30 s CPU time.

Equation 14, for evaluation of the dispersion coefficient, was implemented by integrating independently in each coordinate direction, since the expansion in Eq. 15 is written as the product of functions of r and α. The azimuthal integration was performed analytically and the radial integration numerically using standard adaptive quadrature library routines.

Results and Discussion

The essential results of this work are presented in Figure 2, and represent calculated dispersion coefficients up to appreciably higher values of Dean number than have previously been reported. The ordinate, $(\epsilon/\mathcal{D} - 1)/Pe^2$, is simply the integral in Eq. 14 (apart from a multiplicative constant). Also with the exception of a multiplicative constant, this quantity represents the ratio between the dispersion coefficient in a curved tube and the corresponding one in a straight tube at the same Reynolds number, with both values corrected for the molecular diffusion contribution. As discussed previously, the integral is a function of κ and Sc only, and it is thus plotted as a function of κ with Sc as a parameter for essentially all κ for which flow remains laminar. The dispersion coefficient for any given set of conditions can be found from Figure 2 and Eq. 14; knowledge of three independent dimensionless parameters, for instance Re, δ, and Sc, is required. At low Dean numbers the straight-tube limit, Eq. 1, is approached asymptotically, while at high Dean numbers the value falls approximately as κ^{-1}. For small Schmidt numbers there is, as predicted by Erdogan and Chatwin (1967) and Nunge et al. (1972), a slight increase in dispersion coefficient as κ increases through intermediate values. For larger Schmidt numbers, however, the decrease is monotonic, although inflection points are present (see discussion below). The Erdogan and Chatwin result, also shown in Figure 2, is accurate in predicting the initial deviation from the straight-tube result, but subsequently overpredicts the rate of decrease in the dispersion coefficient. The more general Nunge et al. result is omitted because of its explicit dependence on curvature, but it predicts dispersion coefficients similar to those of Erdogan and Chatwin.

Janssen's (1976) result, which makes use of Dean's (1927) low κ (<15) velocity profiles, is also shown in Figure 2; these results were originally presented as a function of the *single* dimensionless parameter $\kappa^2 Sc$, and have been adapted for use here. Johnson and Kamm's (1986) results are qualitatively similar, but virtually superimposable on our results for $Sc \geq 10$ down to an ordinate value of about 0.0015. Another measure of the agreement of our results with those using Dean's velocity profiles in this part of the parameter space is that a one-decade change in Sc corresponds to a half-decade change in κ on our curves, consistent with dependence on $\kappa^2 Sc$ as the only dimensionless parameter here. Thus the two independent approaches give essentially identical results in this region, in both the initial decline and the asymptotic leveling off.

A comparison of computed dispersion coefficients with the experimental data of van Andel et al. (1964), Trivedi and Vasudeva (1975), and van den Berg and Deelder (1979) is shown in Figure 3. The ordinate is the same as that in Figure 2, and turns

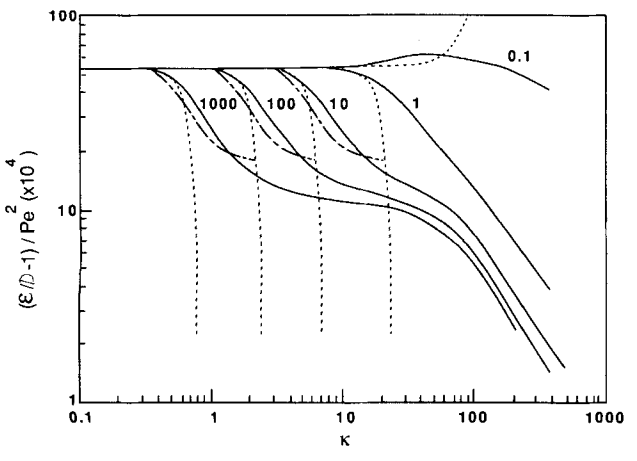

Figure 2. Calculated dispersion coefficients, shown as $(\epsilon/\mathcal{D} - 1)/Pe^2$ vs. κ with Sc as a parameter.

—— This work; —— Erdogan and Chatwin (1967); — · — Janssen (1975)

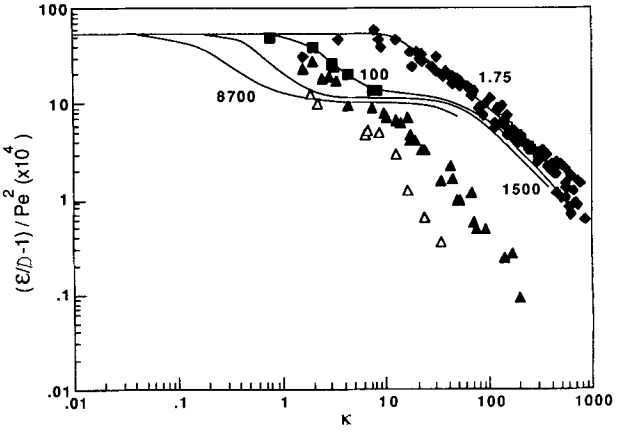

Figure 3. Comparison of calculated dispersion coefficients with experimental results, axes as in Figure 2.

—— This work; ♦ Sc = 1.75 (van Andel et al., 1964); ■ Sc = 110 (van den Berg and Deelder, 1979); ▲ Sc = 1,500, △ Sc = 8,700 (Trivedi and Vasudeva, 1975).

out to be, with the exception of the molecular diffusion contribution to ϵ, the same as the quantity K_c found by Trivedi and Vasudeva (1975) to be best suited to correlating their data. Thus the empirical basis found by Trivedi and Vasudeva for presenting their data is an appropriate one, although in their curves they did not use the correct low Dean number asymptote. This was subsequently corrected by Nigam and Vasudeva (1976). While this method of correlating the data, with κ on the abscissa and Sc as a parameter, is less compact than Janssen's (1976), with $\kappa^2 Sc$ on the abscissa, Janssen's approach is restricted to low κ.

The match between theory and experiment is excellent for the $Sc = 1.75$ data of van Andel et al. and quite good for the $Sc = 110$ data of van den Berg and Deelder. For the $Sc = 1{,}500$ and $Sc = 8{,}700$ data of Trivedi and Vasudeva, however, there are discrepancies at high Dean numbers, mainly in actual values but also in apparent asymptotic slopes at large κ. Similar discrepancies were noted by Johnson and Kamm (1986) even for their more limited Dean number range of interest. The reasons for the differences are not clear, but it is certainly in this part of the parameter space (slow diffusion at high Sc, strong secondary flows at high κ) that both experimental and computational difficulties are most likely to arise.

In experimental work, it is the high Sc, high κ systems that are most susceptible to perturbations because of the significant enhancement of slow diffusive transport that can result from convective disturbances. Such disturbances could result from the finite pitch of experimental tubes (Johnson and Kamm, 1986), and would reduce the observed dispersion coefficient; this would be consistent with the observations in Figure 3. Another consequence of the slow lateral diffusion at high Sc is that longer tubes are needed for the Taylor-Aris limit to be reached. Trivedi and Vasudeva ensured that the concentration profiles from which they computed their dispersion coefficients were consistent with a Fickian dispersion model, but this may not have been sufficient, for a reason that has long been recognized but frequently overlooked in dispersion experiments. This problem, noted by Johnson and Kamm, is that consistency with a dispersion model does not necessarily imply that the corresponding dispersion coefficient has reached its asymptotic steady value. Even if it has, this value is suitable for describing dispersion during further passage along the tube, and not necessarily for describing dispersion between the injection point and the observation point. This factor is apparent in theoretical approaches to evaluating dispersion coefficients, including Taylor's (1953) original one as well as Aris's (1956) method of moments and the developments building on it (Horn, 1971; Brenner, 1980). Interestingly, Taylor's suggested method for using his result, Eq. 1, to estimate diffusivities avoids the problem.

Computational difficulties were encountered at high Schmidt and Dean numbers as well, because of the steep concentration gradients that develop where convective transport is weak (at the walls, along the tube diameter, and at the vortex center). This is why the $Sc = 8{,}700$ line in Figure 3 is incomplete. However, for the results shown there was no reason to doubt that convergence had been attained, and the independent results of Johnson and Kamm agree well with ours even in regions where the discrepancies with experimental results are apparent.

Some of the limiting behavior shown in Figure 2 can be explained using straightforward ordering arguments. All are based on the observation that use of a Fickian dispersion coefficient to describe dispersion induced in the first place by nonuniform axial convection implies $(\epsilon - \mathcal{D}) \sim W^2 t_l$, where t_l is the characteristic time for lateral transport. It follows that $(\epsilon/\mathcal{D} - 1)/Pe^2$, plotted on the ordinate in Figures 2 and 3, goes as $t_l \mathcal{D}/a^2$, and what remains is to estimate t_l in different situations.

At very low Dean numbers the secondary flows are very weak and lateral transport is diffusion-controlled. Thus $t_l \sim a^2/\mathcal{D}$ and $(\epsilon/\mathcal{D} - 1)/Pe^2$ is constant (the Taylor-Aris limit).

At very high Dean numbers the situation is more complicated. It has been argued (McConalogue, 1970) that at the high Dean numbers of interest here the dominant mechanism for lateral transport is convective, a consequence of the increasing intensity of the secondary flow with Dean number. McConalogue's balance of centrifugal and inertial forces suggests that the secondary velocity (U or V) is of order $W\sqrt{\delta}$, from which it follows that $t_l \sim a/W\sqrt{\delta}$ and $(\epsilon/\mathcal{D} - 1)/Pe^2 \sim (\kappa Sc)^{-1}$. The κ dependence is the same as that found by the more detailed computations, but the Sc dependence predicted by the asymptotic analysis appears too strong at high Sc; agreement is better at low Sc.

A more careful examination can be performed by considering the physical interpretation of the diffusion problem, Eqs. 10 to 13, namely, the transport from a source primarily near the tube center to a sink primarily around the periphery. While the secondary flows provide transport between the periphery and the center, there is not necessarily a balance between source and sink around every secondary flow streamline. As evidence of this, Figure 4 shows the normalized net source strength per unit length around individual streamlines as a function of radial position on the radius drawn through the vortex center ($\alpha = 1.52$, 1.48, and 2.05 for $\kappa = 9$, 66, and 373, respectively). These curves were calculated from

$$\frac{\oint \left(w - \frac{\kappa}{2}\right) dl}{\oint dl} \tag{16}$$

where the integration is performed along the closed path of a secondary flow streamline. A contour program was used to pro-

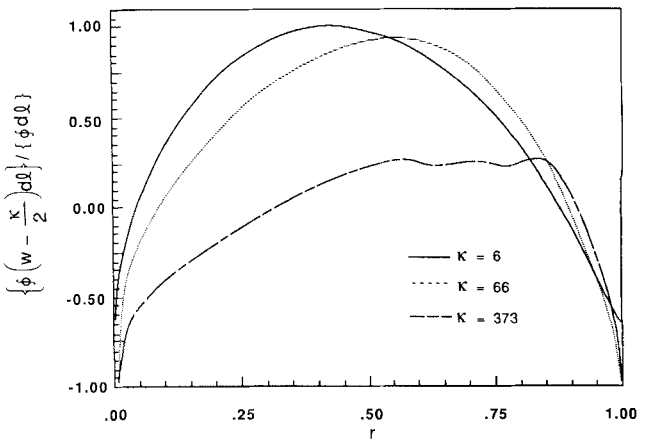

Figure 4. Normalized net source per unit length around individual streamlines, as a function of radial position r.

vide the coordinates (r, α) of points along a particular streamline and a composite trapezoid rule was used for the calculation of the line integral. The peaks are roughly at the vortex centers; each streamline appears, of course, on both sides of the center. As κ increases the vortex center moves toward the outer wall of the tube.

It is clear from the figure that the secondary flow cannot, on its own, provide the required source-to-sink transport, and that diffusion has to play a role. While convective effects on their own certainly have a dispersive effect as well as providing mixing in the cross-sectional plane, the resulting axial profile of the area-average concentration cannot attain its Gaussian shape in the absence of molecular diffusion (see also Brenner, 1980, pp. 127–129). The effect should be significant particularly for high Sc, where diffusion is expected to be limiting. This conclusion is confirmed in two regions of Figure 2, displaying different characteristics. First, for large κ, Figure 4 shows that the characteristic distance for diffusion decreases as the vortex center moves toward the tube wall. This distance, roughly the thickness ℓ of the secondary flow boundary layer, can be estimated from a balance of viscous forces in the boundary layer and centrifugal and intertial forces. This yields $\ell^2 \sim \nu a/W\sqrt{\delta}$, from which t_l for diffusional transport is $\nu a/W\sqrt{\delta}\mathcal{D}$ and the result $(\epsilon/\mathcal{D} - 1)/Pe^2 \sim \kappa^{-1}$ is obtained. This dependence agrees quite well with the high κ, high Sc results. Note that the value of t_l obtained here differs from that for convective transport, obtained earlier, only by a factor of Sc; this confirms that the transition from convection to diffusion control occurs at $Sc \sim 1$.

The second region in which diffusion is limiting despite significant secondary flows is in the leveling off observed at intermediate κ and high Sc. Johnson and Kamm (1986) showed that in the high $\kappa^2 Sc$ limit the concentration profiles in the cross-sectional plane resemble the secondary flow streamlines; this clearly indicates rapid convective transport and slow diffusion. Their asymptotic analysis showed the curved-tube dispersion coefficient to approach 0.2 of the straight-tube value. This result also follows directly from our ordering arguments and Figure 4, where the $\kappa = 6$ result (in the Dean regime) shows the diffusion length to be about $0.45a$. Thus $t_l \sim 0.2a^2/\mathcal{D}$, and the Johnson and Kamm asymptotic result is obtained. The difference between this situation and that at high κ is that in the Dean regime the vortex center remains essentially in the same position for all κ.

A fairly good picture of the physical situation thus emerges. At very low Dean numbers a Taylor-Aris situation prevails, with only diffusive lateral transport because of the very weak secondary flows. At high Dean numbers and low Schmidt numbers, on the other hand, lateral transport is convection-controlled, diffusion being fast. The high Schmidt number behavior is more complicated. The initial decline at low κ seen for high Sc in Figure 2 reflects the increasing role of convection in reducing the predominantly diffusive lateral transport time. For intermediate to high Dean numbers, diffusion is still controlling, but as the diffusion length is reduced by the motion of the vortex center, the functional form of the curved-tube dispersion coefficient changes.

The asymptotic analyses can also be used to estimate the minimum fluid residence time, $\bar{t}$, for which the results of Figure 2 are applicable. This criterion is simply that $\bar{t}$ should be much greater than t_l. Thus at high κ and high Sc, the dimensionless form of $\bar{t}$ used by Trivedi and Vasudeva (1975), $\tau = \bar{t}\mathcal{D}/a^2$, should be much greater than κ^{-1}. Trivedi and Vasudeva's experimental observation was that τ should be greater than $6/Re$ for the dispersion model to be applicable to their results, which differs from our conclusion by only $\sqrt{\delta}$. However, although the experimental concentration profiles seemed to be consistent with the dispersion model, their further development might not be consistent with the same constant Taylor-Aris coefficient. The van Andel et al. (1964) and van den Berg and Deelder (1979) conditions, on the other hand, satisfy the minimum tube length criterion with a much larger margin of error than those of Trivedi and Vasudeva.

Acknowledgment

We are grateful for support provided by the National Science Foundation under Grant No. CBT-8746050, including access to the Pittsburgh Supercomputing Center.

Notation

a = tube radius
A = tube cross section
$\mathcal{D}$ = diffusion coefficient
$K_c = \epsilon\mathcal{D}/4W_m^2a^2$, used by Trivedi and Vasudeva (1975)
ℓ = thickness of secondary flow boundary layer
L = tube length
P_k = Chebyshev polynomial of order k
Pe = Peclet number = $ReSc$
r = dimensionless radial coordinate = r'/a
r' = radial coordinate
R = coil radius
Re = Reynolds number = $2W_ma/\nu$
Sc = Schmidt number = $\nu/\mathcal{D}$
$\bar{t}$ = minimum mean fluid residence time
t_l = characteristic time for lateral transport
u = dimensionless radial velocity = aU/ν
U = radial velocity component
v = dimensionless azimuthal velocity = aV/ν
V = azimuthal velocity component
w = dimensionless axial velocity = $aW\sqrt{\delta}/\nu$
W = axial velocity component
W_m = average axial velocity

Greek letters

α = azimuthal coordinate
β = Dimensionless ψ, Eq. 9
δ = tube curvature = a/R
ϵ = dispersion coefficient
θ = angular coordinate in axial direction
κ = Dean number, $\sqrt{\delta}Re$
ν = kinematic viscosity
τ = dimensionless characteristic time = $\bar{t}\mathcal{D}/a^2$
ψ = fictitious concentration, Eq. 2

Literature Cited

Aris, R., "On the Dispersion of a Solute in a Fluid Flowing through a Tube," *Proc. Roy. Soc. A*, **235**, 67 (1956).

Berger, S. A., L. Talbot, and L.-S. Yao, "Flow in Curved Pipes," *Ann. Rev. Fluid Mech.*, **15**, 461 (1983).

Brenner, H., "Dispersion Resulting from Flow through Spatially Periodic Porous Media," *Phil. Trans. Roy. Soc.*, **297**, 81 (1980).

Daskopoulos, Ph., and A. M. Lenhoff, "Flow in Curved Ducts. I: Bifurcation Structure for Stationary Ducts," *J. Fluid Mech.*, revision submitted for publication.

Dean, W. R., "Note on the Motion of Fluid in a Curved Pipe," *Phil. Mag. (7)*, **4**, 208 (1927).

———, "The Streamline Motion of Fluid in a Curved Pipe," *Phil. Mag. (7)*, **5**, 673 (1928).

Erdogan, M. E., and P. C. Chatwin, "The Effects of Curvature and Buoyancy on the Laminar Dispersion of Solute in a Horizontal Tube," *J. Fluid Mech.*, **29**, 465 (1967).

Gill, W. N., "A Note on the Solution of Transient Dispersion Problems," *Proc. Roy. Soc. A,* **298,** 335 (1967).
Horn, F. J. M., "Calculation of Dispersion Coefficients by Means of Moments," *AIChE J.,* **17** (3), 613 (May, 1971).
Janssen, L. A. M., "Axial Dispersion in Laminar Flow through Coiled Tubes," *Chem. Eng. Sci.,* **31,** 215 (1976).
Johnson, M., and R. D. Kamm, "Numerical Studies of Steady Flow Dispersion at Low Dean Number in a Gently Curving Tube," *J. Fluid Mech.,* **172,** 329 (1986).
Koutsky, J. A., and R. J. Adler, "Minimization of Axial Dispersion by Use of Secondary Flow in Helical Tubes," *Can. J. Chem. Eng.,* **42,** 239 (1964).
Lanczos, C., *Applied Analysis,* Prentice Hall, Englewood Cliffs, NJ, ch. 7 (1956).
McConalogue, D. J., "The Effects of Secondary Flow on the Laminar Dispersion of an Injected Substance in a Curved Tube," *Proc. Roy. Soc. A,* **315,** 99 (1970).
McConalogue, D. J., and R. S. Srivastava, "Motion of a Fluid in a Curved Tube," *Proc. Roy. Soc. A,* **307,** 37 (1968).
Nigam, K. D. P., and K. Vasudeva, "Influence of Curvature and Pulsations on Laminar Dispersion," *Chem. Eng. Sci.,* **31,** 835 (1976).
Nunge, R. J., T.-S. Lin, and W. N. Gill, "Laminar Dispersion in Curved Tubes and Channels," *J. Fluid Mech.,* **51,** 363 (1972).
Pratt, K. C., and W. A. Wakeham, "The Mutual Diffusion Coefficient of Ethanol-Water Mixtures: Determination by a Rapid, New Method," *Proc. Roy. Soc. A,* **336,** 393 (1974).
———, "The Mutual Diffusion Coefficient for Binary Mixtures of Water and the Isomers of Propanol," *Proc. Roy. Soc. A,* **342,** 401 (1975).
Ruthven, D. M., "The Residence Time Distribution for Ideal Laminar Flow in a Helical Tube," *Chem. Eng. Sci.,* **26,** 1113 (1971).
Shetty, V. D., and K. Vasudeva, "Effect of Schmidt Number on Laminar Dispersion in Helical Coils," *Chem. Eng. Sci.,* **32,** 782 (1977).
Taylor, G., "Dispersion of Soluble Matter in Solvent Flowing Slowly through a Tube," *Proc. Roy Soc. A,* **219,** 186 (1953).
———, "Conditions Under Which Dispersion of a Solute in a Stream of Solvent Can be Used to Measure Molecular Diffusion," *Proc. Roy. Soc. A,* **225,** 473 (1954).
Topakoglu, H. C., "Steady Laminar Flow of an Incompressible Viscous Fluid in Curved Pipes," *J. Math. Mech.,* **16,** 1321 (1967).
Trivedi, R. N., and K. Vasudeva, "Axial Dispersion in Laminar Flow in Helical Coils," *Chem. Eng. Sci.,* **30,** 317 (1975).
Van Andel, E., H. Kramers, and A. de Voogd, "The Residence Time Distribution of Laminar Flow in Curved Tubes," *Chem. Eng. Sci.,* **19,** 77 (1964).
Van den Berg, J. H. M., and R. S. Deelder, "Measurement of Axial Dispersion in Laminar Flow through Coiled Capillary Tubes," *Chem. Eng. Sci.,* **34,** 1345 (1979).

Manuscript received Mar. 22, 1988, and revision received July 11, 1988.